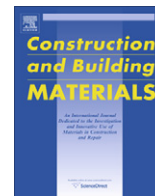




Contents lists available at ScienceDirect

Construction and Building Materials

journal homepage: www.elsevier.com/locate/conbuildmat

Diagonal shear behaviour of unreinforced masonry wallettes strengthened using twisted steel bars

Najif Ismail^{a,*}, Robert B. Petersen^b, Mark J. Masia^b, Jason M. Ingham^a

^a Department of Civil and Environmental Engineering, University of Auckland, Private Bag 92019, Auckland 1142, New Zealand

^b Centre for Infrastructure Performance and Reliability, Faculty of Engineering and Built Environment, University of Newcastle, Callaghan, NSW 2308, Australia

ARTICLE INFO

Article history:
Available online xxx

Keywords:
Masonry
In-plane
Shear
Strengthening
Twisted steel bar
Diagonal testing

ABSTRACT

The in-plane shear behaviour of URM wallettes strengthened using near surface mounted high strength twisted stainless steel reinforcement (TSNSM) was investigated and in particular, the effectiveness of the reinforcing schemes to restrain the diagonal cracking failure mode was studied. A total of 17 URM wallettes, each being 1.2 m × 1.2 m in size, were structurally tested in induced diagonal compression. Of these, 3 wallettes were tested as-built and 14 wallettes were tested after being strengthened using different patterns of TSNSM bars. Several parameters pertaining to the in-plane shear behaviour of strengthened URM walls were investigated, including failure modes, shear strength, maximum drift, pseudo-ductility, and shear modulus. It was inferred from the results that as-built tested wallettes exhibited sudden post-peak strength degradation and failed along a stepped diagonal joint crack, whilst strengthened wallettes failed along distributed diagonal cracks in a more ductile fashion and exhibited a shear strength increment ranging from 114% to 189%.

© 2011 Elsevier Ltd. All rights reserved.

1. Introduction

The majority of fatalities caused by earthquakes in the last one hundred years have resulted from the collapse of unreinforced masonry (URM) buildings [1]. Poor seismic performance of URM buildings was also observed in recent earthquakes such as the 2005 M7.6 Pakistan earthquake [2], the 2008 M7.9 Sichuan earthquake [3], the 2009 M5.8 L'Aquila earthquake [4] and the 2010 M7.1 Darfield earthquake [5]. These experiences have highlighted the vulnerability of URM buildings to damage in the event of a large earthquake, arising from their high seismic mass and limited ductility. But the heritage value associated with these seismically deficient URM buildings typically make their demolition undesirable and their seismic improvement necessary.

During large earthquakes URM walls may be subjected to out-of-plane and in-plane lateral loading as well as vertical compression due to self weight and overburden loads, with in-plane loading governing the global strength and stiffness of the building. The failure mode of URM walls that are subjected to in-plane seismic excitations depends upon wall aspect ratio and the properties of their constituent materials, and are characterised as either flexural controlled or shear controlled [6]. The flexural controlled

mode of failure is characterised by rocking with crushing in plastic hinge zones, usually developed at the lower wall corners or toes, and the shear controlled failure of URM walls is identified by three distinct mechanisms which are bed joint sliding, step joint sliding and diagonal shear cracking [7]. Sliding and rocking failure modes may allow considerable displacement capacity during seismic shaking, and subject to ensuring that collapse is avoided, these deformation modes may be tolerable to some extent [8]. Brittle diagonal shear cracking can be avoided and a sliding or rocking failure mode mobilised by introducing steel reinforcement to URM walls.

Seismic improvement techniques are used to limit damage (by increasing the strength), and/or by prolonging the onset of failure (by increasing the ductility) of the URM building. Many seismic retrofit solutions involving the addition of steel reinforcement have previously been implemented, such as ferrocement overlays, reinforced surface plastering, grouted centre core steel insertion [9] and near surface mounted (NSM) steel insertion [10]. It is believed that the addition of steel reinforcing bars in URM walls allows the strengthened wall to be designed and to perform as a reinforced masonry (RM) wall such that bars yield prior to crushing of masonry. Recent research on RM walls [11–13] extended knowledge pertaining to in-plane seismic behaviour, but that research addressed new concrete masonry construction. Research has also been performed to investigate the structural performance of heritage clay brick masonry walls retrofitted using the near surface mounting (NSM) technique,

* Corresponding author.

E-mail addresses: nism009@aucklanduni.ac.nz (N. Ismail), robert.petersen@newcastle.edu.au (R.B. Petersen), mark.masia@newcastle.edu.au (M.J. Masia), j.ingham@auckland.ac.nz (J.M. Ingham).

which involves the insertion of different types of polymeric reinforcement and deformed steel reinforcement [14–19]. Italian researchers have used this technique to avoid masonry strength degradation due to creep, which is typical in heritage URM construction [20–22]. In the testing program reported here, an improved commercially available grout-bar system was used, which has high corrosion resistance and improved masonry-grout-bar adhesion. To strengthen the test units, twisted steel reinforcement bars were introduced into URM wallettes using the NSM technique, where thin slots are cut into the surface of the masonry and the reinforcement is bonded into the slot using high bond strength thixotropic injectable cementitious grout. The twisted stainless steel reinforcement bars are commercially available and are presently used for applications such as bed joint reinforcement to create deep beams or lintels, structural tying between intersecting structural members, stitching across existing cracks in URM and for strengthening wall ties in existing cavity and veneer masonry construction. In a concurrent study, out-of-plane field testing of URM walls strengthened using twisted stainless steel near surface mounted (TSNSM) reinforcement has been reported [23]. Strengthening of URM arch bridges using a similar bar-grout system has also been reported [24,25]. TSNSM has several advantages as the retrofit application involves minimal disruption and architectural alteration, and the cementitious grout used is easy to work with and is believed to be more compatible with porous heritage URM materials than are the polymeric adhesives that are typically used with fibre reinforced polymer (FRP) reinforcement. Moreover, twisted stainless steel bars have high corrosion resistance and can readily be bent/hooked if additional anchorage is required, the helical profile results in excellent mechanical anchorage over short bond lengths, the application does not increase the seismic weight of the structure, and the system is likely to be accepted by industry due to the proven track record of using steel reinforcement in reinforced masonry construction. It is believed that the cementitious grout has higher fire resistance when compared to its counterpart polymeric adhesion agents, but no experimental validation has been found to support this claim. From discussions with heritage masons, it was also established that the vertical slots may be concealed in architecturally sensitive buildings using a brick face replacement technique, which involves removing the brick surface section and then after insertion of bars, replacing the same colour brick section.

2. Experimental program

A testing program was undertaken to investigate the in-plane performance of URM wallettes seismically strengthened using TSNSM, with the diagonal shear cracking mode of failure investigated in particular. Three as-built and 14 strengthened URM wallettes were tested in induced diagonal compression (in-plane shear).

Table 1
Material properties.

Series		f'_b (N/mm ²)	f_{bt} (N/mm ²)	f'_j (N/mm ²)	f'_m (N/mm ²)	f_t (N/mm ²)
<i>Masonry materials</i>						
1	Value	–	3.6	–	32.1	0.4
	COV	–	21%	–	18%	37%
2	Value	39.4	3.9	1.4	10.7	0.2
	COV	48%	14%	30%	33%	29%
	D (mm)	f_{py} (N/mm ²)	f_{pu} (N/mm ²)	f_{ps} (N/mm ²)	$E_{ps} \times 10^3$ (N/mm ²)	A_s (mm ²)
<i>Reinforcing steel</i>						
1, 2	6	913	1168	697	110–180	7.14
	10	892	1108	470		

Where: f'_b = brick compressive strength; f_{bt} = brick modulus of rupture; f'_j = mortar compressive strength; f'_m = masonry compressive strength; f_t = tensile strength of masonry; f_{py} = specified 0.2% proof stress of reinforcement; f_{pu} = specified ultimate tensile strength of reinforcement; f_{ps} = shear strength of reinforcement; E_{ps} = elastic modulus of reinforcement D = outer bar diameter; and A_s = net cross sectional bar area.

Different orientations of stainless steel NSM reinforcement were used to retrofit the wallettes. The failure modes, load versus displacement response, drift at yield, ultimate drift, pseudo-ductility, shear strength and stiffness of tested wallettes were determined.

2.1. Material properties

Test wallettes were constructed and tested in two series (referred to as series 1 and series 2). Both series used solid (no holes or indentations) extruded clay bricks. Two different mortar compositions, replicating prevalent mortar compositions used in existing modern (series 1) and existing old (series 2) URM construction, were used. Series 1 wallettes were constructed using new bricks being 230 mm long \times 110 mm wide \times 75 mm high, with 10 mm thick mortar joints using a hydraulic cement mortar with a cement:lime:sand ratio (by volume) of 1:1:6 plus an air entraining admixture to the manufacturer's recommended dosage. The admixture was used to increase the mortar workability but also resulted in reduced masonry bond strength. Series 2 wallettes were constructed using salvaged solid clay bricks being 220 mm long \times 105 mm wide \times 90 mm high, with 15 mm thick mortar joints using a hydraulic cement mortar with a cement:lime:sand ratio of 1:2:9 following prevalent masonry construction practices [26].

Masonry modulus of rupture was determined by testing 24 masonry triplets (3 bricks high masonry sub assemblages) for flexural strength in accordance with AS/NZS 4456.15 [27], typically 2 for each wallette. Mortar compressive strength was determined by testing twenty 50 mm mortar cubes in accordance with ASTM C109/C109M-02 [28] and the compressive strength of bricks and masonry were determined in accordance with ASTM C270-03 [29] and ASTM C62-04 [30] respectively, typically in sets of two for each wallette. The results are reported in Table 1 as mean values and associated coefficient of variation (COV). For strengthening, high strength twisted stainless steel bars were used along with a commercially available thixotropic injectable grout (referred to as grout hereafter), which is typically used for TSNSM and was recommended by the manufacturer of the reinforcement. The tensile strength of the twisted steel reinforcing bars was established from testing performed by the manufacturer and the test results are reported in Table 1. Grout cubes were tested after 14 days, resulting in a measured compressive strength value of 44.9 MPa. However, it was established from a literature review of carbon fibre reinforced polymer NSM techniques that the performance of retrofitted walls is largely dependent upon the adhesion of the reinforcement-grout-masonry system. In order to establish the anchorage characteristics of the bar-grout system used, three pull out tests were performed for 2, 3 and 4 brick lengths of straight embedment. Of these three tests, embedment lengths of 3 and 4 brick lengths ultimately resulted in bar rupture and even the 2 brick length embedment resulted in close to the expected rupture load of the bar. The peak force applied on the free end of the reinforcement for 2, 3 and 4 brick length embedment was 7.6 kN, 8.6 kN and 8.7 kN respectively, being close to the nominal specified tensile strength of the 6 mm twisted bar that was used for the tests. Helix unwinding over the bar free length was observed at the conclusion of the pull out testing, with no signs of debonding or grout crushing. The unwinding observed in the pull out tests was attributed to relatively long free lengths between the grips of the testing machine and the masonry anchorage, which is unlikely to happen in actual applications within a strengthened wall.

2.2. Wallette specimens

The experimental program consisted of two series of tests that involved in-plane shear testing of solid clay brick masonry wallettes, with both series strengthened using identical TSNSM bars. Series 1 testing involved diagonal shear (DS) testing of ten single-wythe thick wallettes, constructed using a running bond pattern and series 2 testing involved DS testing of seven 2-wythe thick wallettes, with masonry following a common bond pattern (i.e., one header course after every three stretcher courses). These bond patterns were selected because of their prevalence

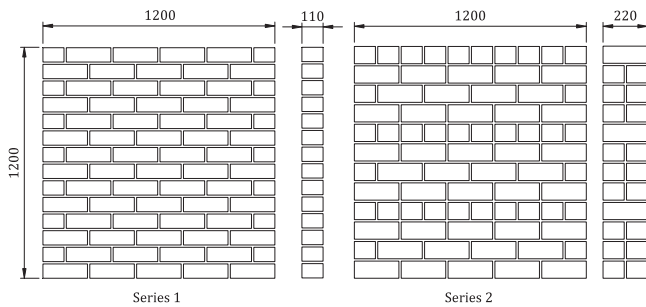


Fig. 1. Wallette geometry and masonry bond patterns.

in existing modern (series 1) and existing old (series 2) URM construction and are shown in Fig. 1. Three wallettes were tested as-built to serve as control wallettes, and 14 wallettes were seismically strengthened prior to testing using different patterns of TSNSM reinforcement (see Fig. 2). As design equations for TSNSM have not yet been developed, the reinforcement patterns used were established from manufacturer recommendations. However, it should be noted that this testing was used more as a proof of concept of a relatively new technology rather than an optimised design assessment, and that further investigation is required in order to optimise reinforcement ratios. The bars were extended to the edges of the wallettes and were finished straight (no bend or cog). For series 1, both faces of each wallette were reinforced to avoid eccentricity and the reinforcing bars were offset on opposite sides of the wallettes to prevent through wall cracking between back to back slots. However, for the majority of heritage URM buildings, retrofit application on the front façade is not desirable and so series 2 involved strengthening on one face only. Test wallettes were given the notation WXC-N or WXS-N, where W refers to wallette, X denotes the test series (1 or 2), C refers to unreinforced control specimens, S refers to the TSNSM retrofit technique and N denotes the test number. Wallette dimensions and details of the retrofit application are shown in Table 2.

2.3. Strengthening procedure

Installation of twisted steel bars first involved grinding of any surface undulations and then cleaning and removal of dust with an air blower. Subsequently, 30 mm deep and 10 mm wide (for diameter 6 mm bars) and 14 mm wide (for diameter 10 mm bars) surface slots (as recommended by the supplier and similar to that used in NSM literature) were cut into the masonry surface using a disc grinder mounted with a dust guard. The cut slots were cleaned with an air blower or

flushed with water. A water based primer was sprayed in the slots by using a blow pump to create a sealing membrane between the porous substrate and the grout, which also enhanced the masonry-grout bond strength. An approximately 10 mm thick bead of grout was injected into the back of the slot using a hand held pointing gun. The twisted steel reinforcing bars were inserted into the slots by pushing them with a finger trowel into the injected bead of grout, and then the slots were filled with grout. Fig. 3 shows photographs of the steel reinforcement used and the retrofit application being performed on a test wallette.

2.4. Test setup

ASTM E-519-02 standard guidelines [31] were used to investigate the in-plane diagonal shear strength. This test procedure provided a simple means of producing diagonal cracking and/or bed joint sliding failure modes and enabled the effectiveness of various strengthening schemes to be evaluated. Displacement controlled loading was applied along the diagonal of the test wallettes at a rate of approximately 0.1 mm/s. Applied diagonal force and the corresponding displacements along both diagonals of the wallettes were recorded.

For series 1, a standard test setup was used (see Fig. 4a) that consisted of a 300 kN hydraulic actuator, 300 kN load cell, loading shoes and four potentiometers. As series 2 wallettes were heavier with lower masonry bond strength, and hence were more vulnerable to damage than series 1 wallettes, a modified test setup was used (see Fig. 4b). The diagonal force was applied to the series 2 wallettes using a 500 kN hydraulic actuator coupled with a 500 kN load cell, and two potentiometers were used to determine the diagonal shortening and elongation. Series 2 wallettes were constructed directly over the steel beams and bricks were placed directly over the steel beam without any mortar interface, allowing sliding to take place and maintaining an unrestrained edge. All potentiometers were attached to test wallettes along the diagonals and had a gauge length of 1414 mm.

3. Experimental results and discussion

3.1. Crack patterns

Testing was continued until either the post-peak shear stress degraded to half of the maximum shear strength, or the equivalent lateral drift reached 1%. The as-built wallettes (W1C-1, W1C-2 and W2C-3) exhibited an approximately linear behaviour up to first cracking and then failed suddenly along a diagonal step joint when they reached their diagonal tensile strength (Fig. 5a and e).

For the strengthened wallettes with vertically aligned reinforcement, diagonal cracking initiated close to peak load but was

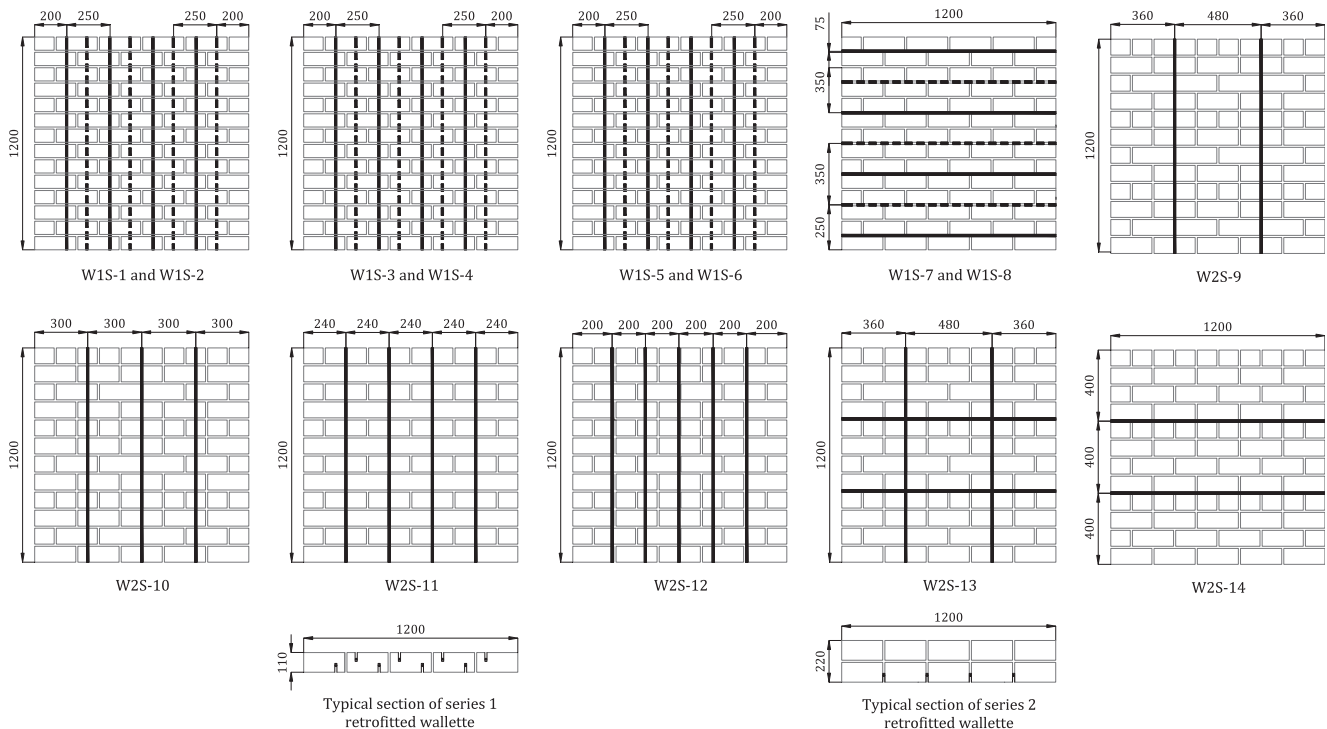


Fig. 2. Strengthening details (dashed lines represent bars installed on rear face).

Table 2
Wallette dimensions and retrofit details.

Series	Wallette	Wallette dimensions (mm)			Retrofit details	
		<i>H</i>	<i>B</i>	<i>t</i>	Strengthened with (number of faces strengthened shown in parenthesis)	Pattern
1	W1C-1	1200	1200	110	–	–
	W1C-2	1200	1200	110	–	–
	W1S-1	1200	1200	110	4 slots equally spaced with 1T6 in each slot (2)	V
	W1S-2	1200	1200	110	4 slots equally spaced with 1T6 in each slot (2)	V
	W1S-3	1200	1200	110	4 slots equally spaced with 2T6 in each slot (2)	V
	W1S-4	1200	1200	110	4 slots equally spaced with 2T6 in each slot (2)	V
	W1S-5	1200	1200	110	4 slots equally spaced with 2T10 in each slot (2)	V
	W1S-6	1200	1200	110	4 slots equally spaced with 2T10 in each slot (2)	V
2	W1S-7	1200	1200	110	4 slots on one face and 3 slots on the other face with 1T6 in each slot (2)	HL
	W1S-8	1200	1200	110	4 slots on one face and 3 slots on the other face with 1T6 in each slot (2)	HL
	W2C-3	1200	1200	220	–	–
	W2S-9	1200	1200	220	2 slots equally spaced with 1T6 in each slot (1)	V
	W2S-10	1200	1200	220	3 slots equally spaced with 1T6 in each slot (1)	V
	W2S-11	1200	1200	220	4 slots equally spaced with 1T6 in each slot (1)	V
	W2S-12	1200	1200	220	5 slots equally spaced with 1T6 in each slot (1)	V
	W2S-13	1200	1200	220	4 slots with 1T6 in each slot (1)	G
W2S-14	1200	1200	220	2 slots equally spaced with 1T6 in each slot (1)	HL	

Where: *H* = wallette height; *B* = wallette length; *t* = wallette thickness; HL = horizontal; V = vertical; G = grid; and T = high strength twisted stainless steel bar.

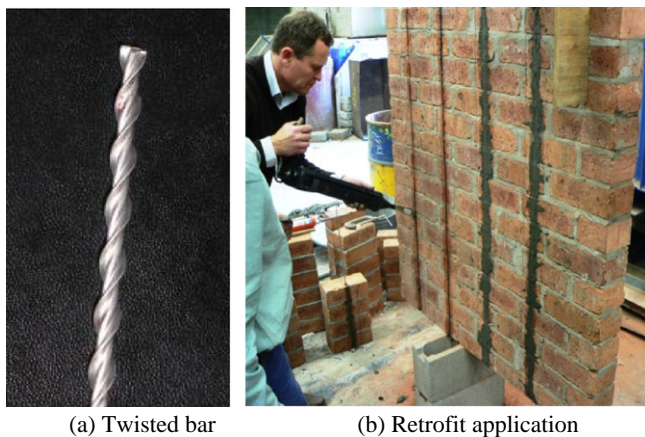


Fig. 3. Photographs of test wallette preparation.

restrained by the reinforcement, resulting in more ductile modes of failure than observed for the URM control specimens. The resulting failure modes involved distributed diagonal cracking across the compressed diagonal region of the wallettes (Fig. 5c and g). In the vicinity of major diagonal cracks, after large displacements, there was considerable local crushing of the masonry and cementitious grout adjacent to the reinforcing bars (Fig. 5d). The twisted steel NSM bars held the cracked masonry together and restrained the shear induced dilation mechanism which developed along the sliding portions of the cracking surfaces. This restraint to dilation increased the frictional resistance of the cracks, resulting in increased load and displacement capacity. Any dowel action was likely to be insignificant due to excessive local bending of the reinforcing bars across the shear cracks (Fig. 5d). Despite the shear cracks crossing the bars close to the edges of the wallettes, bar slippage or reinforcement debonding was not observed in the testing, confirming that there was sufficient mechanical bond between the reinforcement and masonry over short embedment lengths.

In test wallettes W1S-1 and W1S-2, during and after the tests, it was observed that several of the bars had ruptured, but no bar rupture was observed in the other tests. All strengthened wallettes failed with diagonal cracks except W1S-7 and W1S-8 (series 1 – horizontally aligned reinforcement), which developed diagonal cracks but ultimately failed by sliding along an unstrengthened horizontal mortar joint (see Fig. 5b). Test wallette W2S-14

(Fig. 5f) was also strengthened using a horizontal reinforcement pattern. However, when compared to W1S-7 and W1S-8, wallette W2S-14 had additional compression stress normal to the mortar bed joints due to wallette self weight, and exhibited a diagonal cracking failure mode. Visible out-of-plane bending of test wallettes having high reinforcement ratios on one face only (W2S-11 and W2S-12) was also observed in the testing.

3.2. Shear stress–drift response

The experimentally measured diagonal force, *P*, was transformed into shear stress, *t*, using Eq. (1), where *t* is wallette thickness, *B* is wallette length, *H* is wallette height, and *a* is the angle between the wallette diagonal and the horizontal axis. Measured drift values, *d*, were calculated using Eq. (2), where *DS* is diagonal shortening along the axis of applied force, *DL* is diagonal elongation measured perpendicular to the axis of applied force, and *g* is the gauge length.

$$m = \frac{P \cos \alpha}{0.5t(H + B)} \quad (1)$$

$$d = \frac{DS + DL}{2g} (\tan \alpha + \cot \alpha) \quad (2)$$

A maximum allowable drift limit of 0.5–0.6% is typically specified in design codes [32,33] for URM walls, and hence curves were plotted to a maximum drift of 1.0% (see Fig. 6a–l). The force–displacement response of the as-built tested wallettes exhibited sudden strength degradation once cracking had propagated. A linear–elastic behaviour up to cracking and then a gradual decrease in the post-peak strength was observed in all strengthened wallettes (see Fig. 6a–k), except for W1S-7 and W1S-8 which failed by sudden sliding failure along a horizontal mortar joint (see Fig. 6e). It is noted that typical URM walls are loaded axially due to their self weight and overburden loads, and that bed joint sliding failure modes may not lead to sudden complete loss of strength as observed here.

3.3. Shear strength

Maximum shear stress values are listed in Table 3, and are also expressed as a ratio of the shear strength of the corresponding as-built wallette. As-built tested URM wallettes W1C-1 and W1C-2

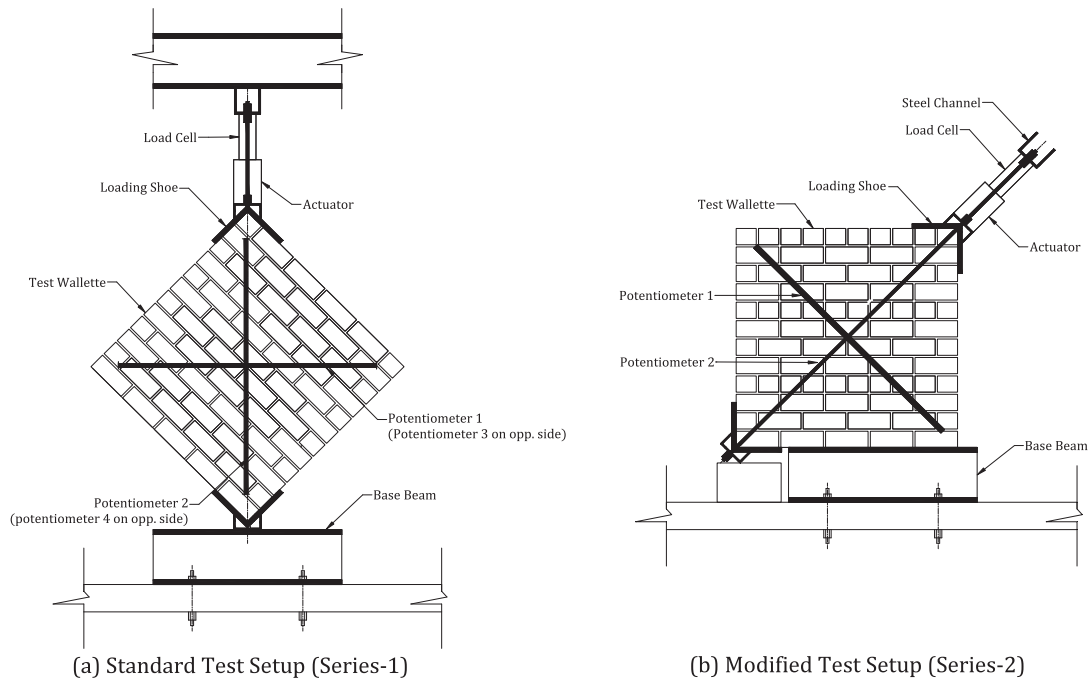


Fig. 4. Test setup.

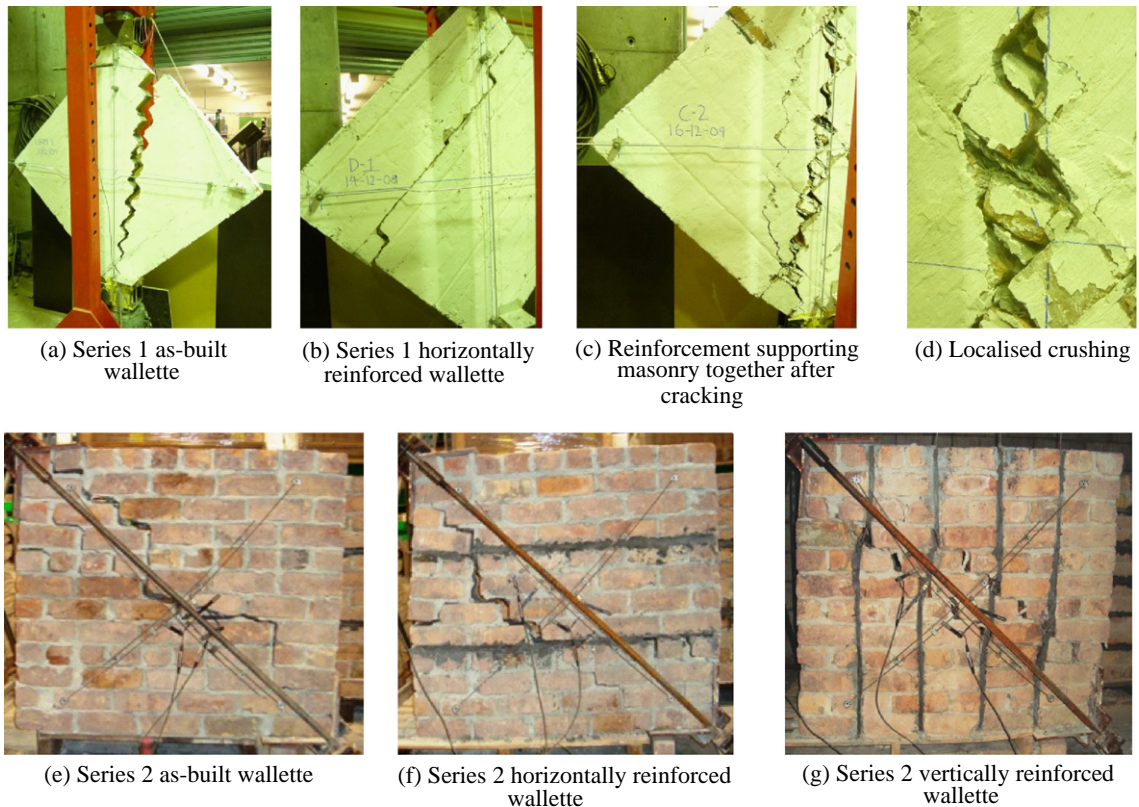


Fig. 5. Crack patterns and photographs of tested wallettes.

behaved almost linearly up to peak load and then failed suddenly at small deformations with a diagonal cracking failure mode. Test wallette W2C-3 cracked diagonally along the mortar step joint and upon further application of the diagonal displacement the upper portion of the wallette slid in the horizontal direction. All three reinforcement patterns resulted in higher shear strength

values, on average, than was measured for the as-built URM control specimens, with the combined horizontal and vertical grid pattern resulting in the largest strength increase. Furthermore, the reinforcement restrained the opening of diagonal cracks which developed during loading, allowing the wallettes to undergo large displacement while continuing to support significant load. All

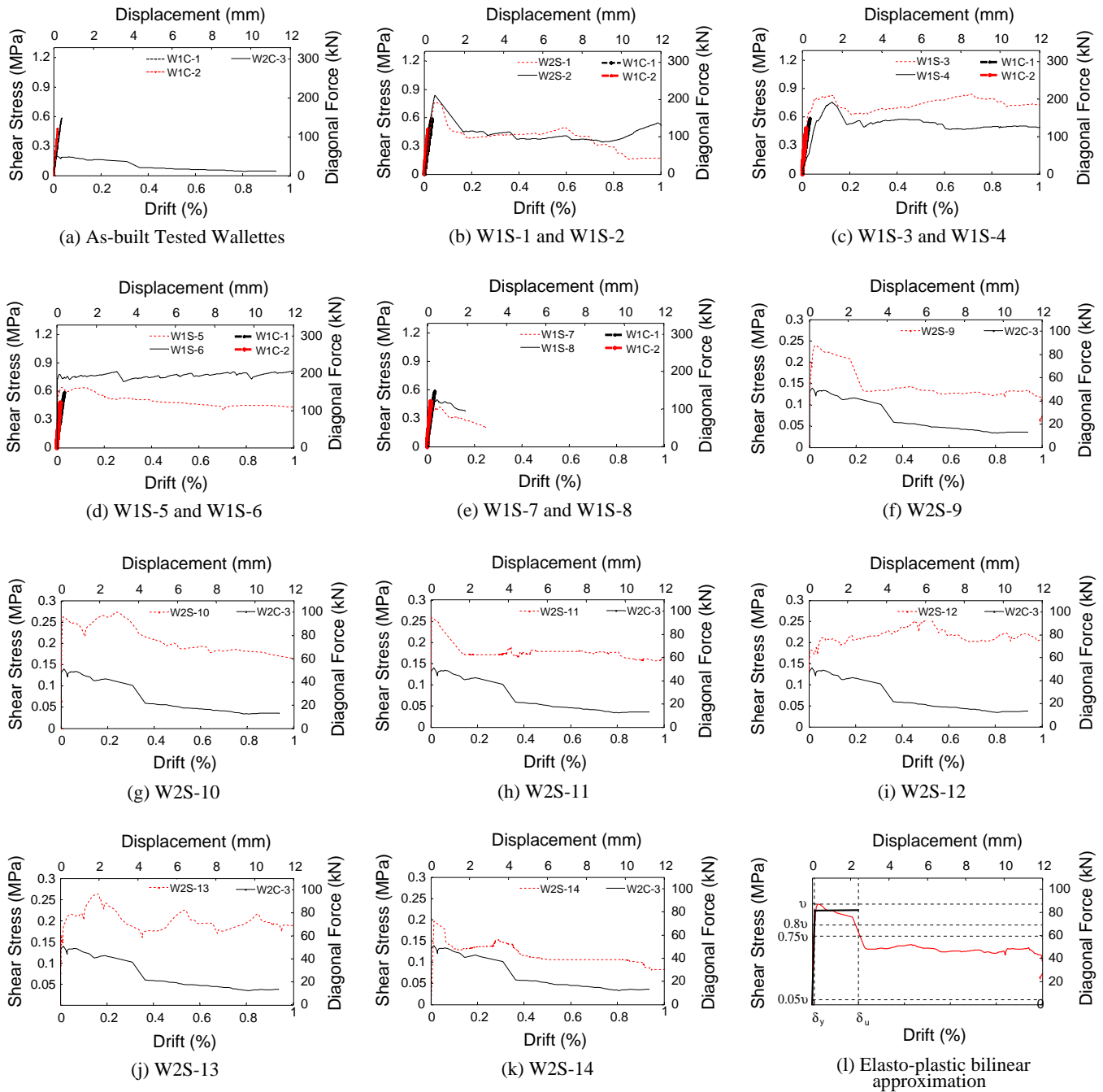


Fig. 6. Shear stress–drift plots.

strengthened wallettes except W1S-7 and W1S-8 continued to resist load at the conclusion of testing. Specimens W1S-7 and W1S-8 failed at loads lower than measured for the as-built URM control specimens but this was identified to result from the masonry that was used to construct these two specimens having a bond strength that was significantly lower than the series 1 mean value [34]. The reduced bond strength of these two wallettes was either due to a mistake in mortar proportion or due to a longer mixing time than for other mortar batches, resulting in more air voids in the mortar.

3.4. Pseudo-ductility

Materials that can deform beyond the elastic range with a gradual drop in capacity are said to be ductile. In the event of an earthquake, buildings undergo lateral displacement and the ability of a

building to deform without collapsing is termed structural ductility. As the shear stress–drift plots for tested wallettes did not have a distinct yield point, pseudo-ductility was determined using an elasto-plastic bilinear approximation (see Fig. 6l). The ultimate drift, d_u , was determined as the drift value when the shear strength degraded to $0.8t$ and the yield drift, d_y , was determined such that the area under the bilinear curve was the same as that under the experimental curve. The values of ultimate and yield drift are reported in Table 3 and the pseudo-ductility, I , was determined using the equation.

$$I = \frac{d_u}{d_y} \quad (3)$$

The large increase in pseudo-ductility for strengthened wallettes was attributed to reinforcement holding the brick masonry together and distributing stresses over larger areas. Pseudo-ductility

Table 3
Test results.

Series	Wallette	$q_h \times 10^{-3}$	$q_v \times 10^{-3}$	P_{max} (kN)	F_{max} (kN)	t_{max} (N/mm ²)	t/t_o (%)	$d_y \times 10^{-3}$ (mm)	$d_u \times 10^{-3}$ (mm)	l	$G \times 10^3$ (N/mm ²)	$E \times 10^3$ (N/mm ²)
1	W1C-1	0.00	0.00	157.0	111.0	0.84	–	0.3	0.3	1	2.8	7.0
	W1C-2	0.00	0.00	129.0	91.2	0.69	–	0.2	0.2	1	3.5	8.6
	W1S-1	0.00	0.43	193.0	136.5	1.03	135	0.4	0.8	2	2.6	6.4
	W1S-2	0.00	0.43	212.0	149.9	1.14	148	0.3	1.0	3	3.8	9.5
	W1S-3	0.00	0.87	212.0	149.9	1.14	148	0.3	1.9	6	3.8	9.5
	W1S-4	0.00	0.87	192.0	135.7	1.03	134	0.8	1.7	2	1.3	3.2
	W1S-5	0.00	1.79	163.0	115.2	0.87	114	0.1	2.6	26	8.7	21.8
	W1S-6	0.00	1.79	209.0	147.8	1.12	146	0.1	19.8	198	11.2	28.0
2	W1S-7	0.38	0.00	105.0	74.2	0.56	73	0.1	0.8	8	5.6	14.0
	W1S-8	0.38	0.00	124.0	87.7	0.66	87	0.3	1.3	4	2.2	5.5
	W2C-3	0.00	0.00	51.0	36.0	0.14	–	0.1	0.7	7	1.0	2.5
	W2S-9	0.00	0.11	87.0	61.5	0.23	171	0.3	1.7	6	0.7	1.7
	W2S-10	0.00	0.16	93.4	61.1	0.25	183	0.2	3.5	18	1.2	2.9
	W2S-11	0.00	0.22	94.0	66.4	0.25	184	0.2	9.2	46	1.3	3.1
	W2S-12	0.00	0.27	94.6	66.9	0.25	186	0.1	11.2	112	2.5	6.3
	W2S-13	0.11	0.11	96.2	68.0	0.26	189	0.4	3.6	9	0.7	1.6
W2S-14	0.11	0.00	71.6	50.6	0.19	140	0.3	8.7	29	0.8	2.0	

Where: q_h = horizontal reinforcement ratio; q_v = vertical reinforcement ratio; P_{max} = maximum applied diagonal force; F_{max} = maximum horizontal shear force; t_{max} = maximum shear stress; d_y = % drift at yield; d_u = % drift at failure (corresponding to 0.8t); l = pseudo-ductility; G = modulus of rigidity; E = modulus of elasticity; and t/t_o = ratio of the shear strength to that of the as-built wallette.

is often used in demand capacity phase diagram based design, where a pushover curve is generated for the building [35,36]. Referring to Table 3, it is noted that the ductility factor was determined using induced diagonal cracking and is highly sensitive to the calculated yield drift, d_y , which for the current tests showed considerable variability and for many of the tests was calculated as a very small value. The large variations in observed d_y were attributed to redistribution of stresses and deformations throughout the highly heterogeneous material during the pre-peak loading phase, resulting in the displacement that was measured along the compression diagonal being not representative of the true elastic drift.

3.5. Stiffness

The modulus of rigidity, G, was determined as the secant modulus between $0.05t_{max}$ and $0.75t_{max}$ of the shear stress–shear strain plots. The stiffness of test wallettes was quantified by the elastic modulus, E, which is related to the modulus of rigidity, G. For each wallette a corresponding elastic modulus was calculated as:

$$E = 2G(1 + p) \quad (4)$$

where G = shear modulus and p = Poisson's ratio (adopting $p = 0.25$). The more lightly reinforced wallettes had stiffness values that were lower than their counterpart non-strengthened wallettes (possibly due to cut grooves in the surface of the wallettes), but the wallettes with higher reinforcement ratios were more stiff. The elastic moduli determined for all test wallettes are reported in Table 3.

4. Conclusions

The in-plane shear behaviour of URM wallettes strengthened using near surface mounted high strength twisted stainless steel reinforcement bars was investigated. The effectiveness of the reinforcing schemes to restrain the diagonal cracking failure mode was studied. The study considered horizontal, vertical and grid pattern reinforcement applied to single-wythe thick and two-wythe thick wallettes. Parameters pertaining to seismic behaviour were determined, including shear strength, drift capacity, pseudo-ductility, shear modulus and elastic modulus. The results were compared to those obtained from testing as-built URM wallettes. The key findings of the experimental program are:

1. The improvement in shear strength (i.e., t/t_o) for strengthened wallettes ranged from 114% to 189% except for W1S-7 and W1S-8, which were strengthened using a horizontal pattern and showed decreased shear strength. The latter was due to the masonry bond strength for these two specimens being significantly lower than the series mean.
2. The horizontal reinforcement scheme was effective in bridging diagonal cracks which formed close to peak load, and allowed the wallettes to deform further until ultimate failure occurred. This behaviour resulted in a smaller increase in shear strength, on average, when compared to other reinforcement schemes, but a large increase in pseudo-ductility was observed.
3. The vertical and grid reinforcement schemes performed the best in terms of increases in strength and displacement capacity. The presence of vertical reinforcement restrained opening of the diagonal cracks which developed during loading, allowing the wallettes to undergo large displacement while continuing to support significant load, and resulted in a larger shear strength increase than when using the horizontal reinforcement scheme.
4. The effect of increasing the vertical reinforcement percentage was to reduce the post-peak drop in load and hence increase the ductility of the wallettes.
5. All strengthened wallettes (except those that were strengthened using horizontal schemes) displayed ductile failure modes and continued to resist load at the completion of testing.
6. The primary reinforcement mechanism for vertically aligned reinforcement was restraint to shear induced dilation which resulted in increased frictional shear resistance along the shear cracks. Dowel action was likely insignificant due to the excessive local bending of the reinforcing bars across the shear cracks.
7. The helical profile of the stainless steel reinforcing bars resulted in excellent mechanical bond between the reinforcement and masonry over short bonded lengths.

Acknowledgments

Financial support for this testing was provided by the New Zealand Foundation for Research Science and Technology via Project UOAX0411 and the Australian Research Council via discovery Project 0879592. Helifix (Australia) Pty Ltd supplied materials

and provided assistance with testing. The Higher Education Commission of Pakistan provided funding for the doctoral studies of the first author.

References

- [1] Coburn A, Spence R. Earthquake Protection. New York: Wiley; 1992.
- [2] Bothara JK, Hicisiylmaz KMO. General observations of building behaviour during the 8th October 2005 Pakistan earthquake. *Bull NZ Soc Earthquake Eng* 2008;41(4):209–33.
- [3] Zhao T, Zhang X, Tian Z. Analysis of earthquake damage to masonry school buildings in Wenchuan earthquake. *World Inf Earthquake Eng* 2009;25(3):150–8.
- [4] Kaplan H, Bilgin H, Yilmaz S, Binici H, Öztas A. Structural damages of L'Aquila (Italy) earthquake. *Nat Hazards Earth Syst Sci* 2010;10(3):499–507.
- [5] Dizhur D, Ismail N, Knox C, Lumantarna R, Ingham JM. Performance of unreinforced and retrofitted masonry buildings during the 2010 Darfield earthquake. *Bull NZ Soc Earthquake Eng* 2010;43(4):321–39.
- [6] Priestley MJN. Seismic behaviour of unreinforced masonry walls. *Bull NZ Soc Earthquake Eng* 1985;18(2):191–205.
- [7] Magenes G, Calvi GM. In-plane seismic response of brick masonry walls. *Earthquake Eng Struct Dyn* 1997;26(11):1091–112.
- [8] Oyarzo-Vera C, Griffith MC. The Mw 6.3 Abruzzo (Italy) earthquake of April 6th, 2009: onsite observations. *Bull NZ Soc Earthquake Eng* 2009;42(4):302–7.
- [9] Abrams D, Smith T, Lynch J, Franklin S. Effectiveness of rehabilitation on seismic behavior of masonry piers. *J Struct Eng ASCE* 2007;133(1):32–43.
- [10] Asplund SO. Strengthening bridge slabs with grouted reinforcement. *J Am Concr Inst* 1949;20(6):397–406.
- [11] Voon KC, Ingham JM. Experimental in-plane shear strength investigation of reinforced concrete masonry walls. *J Struct Eng ASCE* 2006;132(3):400–8.
- [12] Voon KC, Ingham JM. Design expression for the in-plane shear strength of reinforced concrete masonry. *J Struct Eng ASCE* 2007;133(5):706–13.
- [13] Voon KC, Ingham JM. Experimental in-plane strength investigation of reinforced concrete masonry walls with openings. *J Struct Eng ASCE* 2008;134(5):758–68.
- [14] De Lorenzis L, Teng JG. Near-surface mounted FRP reinforcement: an emerging technique for strengthening structures. *Composites Part B* 2007;38(2):119–43.
- [15] Turco V, Secondin S, Morbin A, Valluzzi MR, Modena C. Flexural and shear strengthening of un-reinforced masonry with FRP bars. *Compos Sci Technol* 2006;66(2):289–96.
- [16] Valluzzi MR, Tinazzi D, Modena C. Shear behavior of masonry panels strengthened by FRP laminates. *Constr Build Mater* 2002;16(7):409–16.
- [17] Korany Y, Drysdale R. Load-displacement of masonry panels with unbonded and intermittently bonded FRP. II: analytical study. *J Compos Constr* 2007;11(1):24–32.
- [18] Petersen RB, Masia MJ, Seracino R. In-plane shear behavior of masonry panels strengthened with NSM CFRP strips. I: experimental investigation. *J Compos Constr* 2010;14(6):754–63.
- [19] Willis CR, Seracino R, Griffith MC. Out-of-plane strength of brick masonry retrofitted with horizontal NSM CFRP strips. *Eng Struct* 2010;32(2):547–55.
- [20] Modena C, Valluzzi MR. Repair techniques for creep and long-term damage of massive structures. In: Brebbia Carlos, editor. Structural studies, repairs and maintenance of Heritage Architecture VIII. Southampton, UK: Wessex Institute of Technology Press; 2003. p. 141–50.
- [21] Valluzzi MR, Tinazzi D, Modena C. Strengthening of masonry structures under compressive loads by FRP strips: local–global mechanical behaviour. *Sci Eng Compos Mater* 2005;12(3):203–18.
- [22] Valluzzi MR, Binda L, Modena C. Mechanical behaviour of historic masonry structures strengthened by bed joints structural repointing. *Constr Build Mater* 2005;19(1):63–73.
- [23] Ismail N, Oyarzo Vera C, Ingham JM. Field testing of URM walls seismically strengthened using twisted steel inserts. X Chilean Conference on Seismology and Earthquake Engineering. Santiago, Chile; 2010.
- [24] Chen Y, Ashour AF, Garrity SW. Modified four-hinge mechanism analysis for masonry arches strengthened with near-surface reinforcement. *Eng Struct* 2007;29(8):1864–71.
- [25] Chen Y, Ashour AF, Garrity SW. Moment/thrust interaction diagrams for reinforced masonry sections. *Constr Build Mater* 2008;22(5):763–70.
- [26] AS Committee 3700. Masonry structures. Standards Australia; 2001.
- [27] AS/NZS Committee 4456.15. Methods of test for masonry units, segmental pavers and flags – determining lateral modulus of rupture. Standards Australia; 2003.
- [28] ASTM Committee C109/C109M-02. Standard test method for compressive strength of hydraulic cement mortars. American Society for Testing and Materials International; 2002.
- [29] ASTM Committee C270-03. Standard test method for compressive strength of masonry prisms. American Society for Testing and Materials International; 2003.
- [30] ASTM Committee C62-04. Standard specification for building brick-solid masonry units made from clay or shale. American Society for Testing and Materials International; 2004.
- [31] ASTM Committee E-519-02. Standard test method for diagonal tension (shear) in masonry assemblages. American Society for Testing and Materials International; 2002.
- [32] BS. Design of structures for earthquake resistance (BS EN 1998-3:2005). British Standards Institution; 2005.
- [33] TSB Committee E30. Earthquake resistant design: national construction code. Technical Standard for Buildings (Lima); 1998.
- [34] Masia MJ, Petersen RB, Konthesingha C, Lahra J. In-plane shear behaviour of masonry panels strengthened with stainless steel high stress reinforcement. In: 8th International masonry conference. Dresden, Germany; 2010.
- [35] Chopra AK, Goel RK. Capacity-demand-diagram methods based on inelastic design spectrum. *Earthquake Spectra* 1999;15(4):637–56.
- [36] Freeman SA. The capacity spectrum method as a tool for seismic design. In: 11th European conference on earthquake engineering. Paris, France; 1998.